Electronic Structure of the Tris(1,3-diphenyltriazenido)aluminum Radical Anion: A Theoretical and Experimental ESEEM and EPR Study

Christian T. Farrar, John T. Leman, Sarah C. Larsen, Janet Braddock-Wilking, David J. Singel,*,† and Andrew R. Barron*

Contribution from the Department of Chemistry, Harvard University, Cambridge, Massachusetts 02138

Received February 22, 1994®

Abstract: Multifrequency ESEEM (electron spin echo envelope modulation) and EPR spectroscopies are employed to elucidate the electronic structure of the monoradical anion of tris(1,3-diphenyltriazenido)aluminum, $[Al(dpt)_3]^-$, which is obtained by the chemical reduction of $Al(dpt)_3$. Analysis of the EPR and ESEEM spectra obtained for various isotope-labeling combinations, including ^{15}N isotope labeling of either the 1,3 (flanking) or 2 (central) positions of the diphenyltriazenide ligands, allows for the detailed study of the electronic structure of the radical anion. EPR spectra of the ^{15}N-labeled derivatives clearly indicate that the radical anion complex is ligand-centered with strong hyperfine couplings to the nitrogen nuclei of a single triazenide ligand observed. However, detailed analysis of the strong hyperfine couplings exhibited in the EPR spectra is prevented by the lack of resolution. A multifrequency ESEEM spectroscopy study was undertaken in order to resolve the weakly coupled nuclei obscured in the EPR spectra by the inhomogeneous line broadening. A very weak coupling to the aluminum center is manifested in the ESEEM spectra, further supportive of the ligand-centered nature of the radical anion complex. Also evident from the ESEEM spectra are three distinguishable types of nitrogen nuclei: weak, anisotropically coupled central and flanking nitrogens and weak, isotropically coupled (*ca.* 1 Gauss) flanking nitrogens. *Ab initio* calculations were performed in order to aid in the assignment of the nuclear hyperfine couplings observed in the ESEEM and EPR spectra to specific nitrogen positions on the triazenide rings. Together, the EPR, ESEEM, and *ab initio* calculations give a coherent picture of the electron spin density distribution and bonding in the radical anion $[Al(dpt)_3]^-$. Reduction of the aluminum complex results in localization of the electron onto the $p-\pi^*$ molecular orbitals of one of the three diphenyltriazenide ligands.

Introduction

In the preceding paper, we reported on the synthesis and characterization of a homologous series of aluminum radical anion complexes $[Al(dpt)_3]^{n-}$ (Hdpt = 1,3-diphenyltriazene; n = 1, 2, and 3; I).[1] There has been disagreement in previous studies of paramagnetic group 13 coordination complexes as to the formal oxidation state of the metal atom (*i.e.*, whether one obtains a metal[2] or ligand-centered[3] radical upon reduction[4]) and the exact electronic structure of the resulting radical. On the basis of a small contact shift observed in the ^{27}Al NMR spectrum, the observation of a reduced nitrogen environment in the X-ray photoelectron spectrum (XPS), and the triplet structure in the frozen glass EPR spectrum, we have proposed the unpaired electron in $[Al(dpt)_3]^-$ to be primarily ligand-centered, with aluminum in the +3 formal oxidation state.[1] The qualitative nature of these studies, however, leaves this question not entirely resolved. In addition, it is of interest to characterize the electron spin density distribution on the radical anion complexes $[Al(dpt)_3]^{n-}$, specifically, to determine whether the spin density is coherently delocalized over all three ligands or localized onto a single triazenide ligand.

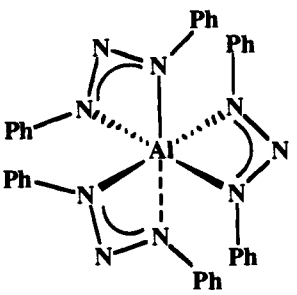

$Al(dpt)_3$

(I)

The experimental approach we have adopted for probing the electronic structure of the monoradical $[Al(dpt)_3]^-$ involves the determination of the electron−nuclear hyperfine couplings, which reflect the electron spin density distribution in the molecule. Couplings that are large enough to impart structure in the EPR spectrum are determined by detailed simulations of the observed spectra; assignments of the hyperfine couplings to particular nuclei are verified by substitution of selected isotopes. Weaker hyperfine couplings that are concealed by the inhomogeneous broadening of EPR spectra are revealed by

* Authors to whom correspondence should be addressed.

† Current address: Department of Chemistry, Montana State University, Bozeman, MT 59717.

® Abstract published in *Advance ACS Abstracts,* January 15, 1995.

(1) Braddock-Wilking, J.; Leman, J. T.; Farrar, C. T.; Larsen, S. C.; Singel, D. J.; Barron, A. R. *J. Am. Chem. Soc.* **1995**, *117*, 1736.

(2) See, for example: Cloke, F. G. N.; Dalby, C. I.; Henderson, M. J.; Hitchcock, P. B.; Kennard, C. H. L.; Lamb, R. N.; Ratson, C. L. *J. Chem. Soc., Chem. Commun.* **1990**, 1394.

(3) See, for example: Kaim, W.; Matheis, W. *J. Chem. Soc., Chem. Commun.* **1991**, 597.

(4) For a recent review of low-valent and paramagnetic compounds of aluminum, see: Barron, A. R. In *Coordination Chemistry of Aluminum*; Robinson, G. H., Ed.; VCH: New York, 1993; p 123.

0002-7863/95/1517-1746$09.00/0

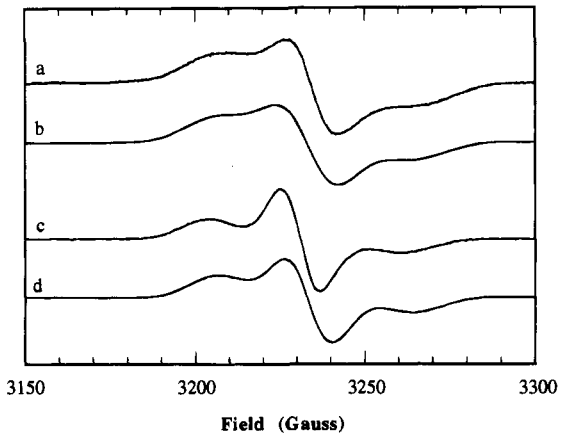

Figure 1. Frozen solution (77 K) EPR spectra of the sodium (a) and PPN (c) salts of the monoreduced radical anion $[Al(dpt)_3]^-$ along with their respective simulations (b and d). The simulations were obtained assuming coupling to three nitrogens with hyperfine couplings of $A_{||}$ = 5 G and $A_\perp$ = 2 G and $A_{||}$ = 30 G and $A_\perp$ = 5 G and an axially symmetric **g** tensor with principal values $g_\perp = 2.0000$ and $g_{||} = 2.0023$. Gaussian line broadenings of 5 and 7 Gauss are used in simulations (d) and (b), respectively.

ESEEM (electron spin echo envelope modulation)[5] spectroscopy. The measured hyperfine couplings are interpreted with guidance from *ab initio* calculations of the electronic structure. From this joint experimental and theoretical investigation, a detailed, yet simple, picture of the electronic structure in the $[Al(dpt)_3]^-$ radical anion is obtained.

Results and Discussion

EPR Spectroscopy. The frozen solution (77 K, THF) EPR spectra of the sodium and bis(triphenylphosphine)iminium (PPN) salts of the monoreduced radical anion $[Al(dpt)_3]^-$ are shown in spectral lines (a) and (c), respectively, of Figure 1. We note that the spectrum exhibited by the $[Al(dpt)_3]^-$ anion, irrespective of the identity of the cation, is qualitatively similar to that generically observed for nitroxide spin-labels[6] and thus suggests extensive spin density on a ligand nitrogen. As is evident in Figure 1c, the spectral resolution is only slightly enhanced when the sodium cation is replaced with PPN, a large countercation. This effect is usually assigned to an increased cation−anion segregation. However, such an effect may be diminished by the dilution of the ESR sample [$(1-5) \times 10^{-3}$ mol L^{-3}].[1]

The experimental spectra are readily simulated (Figure 1b,d) by assuming hyperfine couplings to three nitrogens with coaxially symmetric electron Zeeman (**g**) and nitrogen hyperfine (**A**) matrices and a Gaussian line broadening of 5 G for the PPN cation spectrum (Figure 1d) and 7 G for the sodium cation spectrum (Figure 1b). The parameter values that give the best simulations are $g_\perp = 2.0000$ and $g_{||} = 2.0023$ and hyperfine couplings of $A_{||}$ = 5 G and $A_\perp$ = 2 G for two equivalent nitrogens and $A_{||}$ = 30 G and $A_\perp$ = 5 G for a more strongly coupled, single nitrogen. The large hyperfine coupling $A_{||}$ = 30 G is plainly apparent in the EPR spectra of Figure 1; the coupling to the other two nitrogens, the perpendicular component

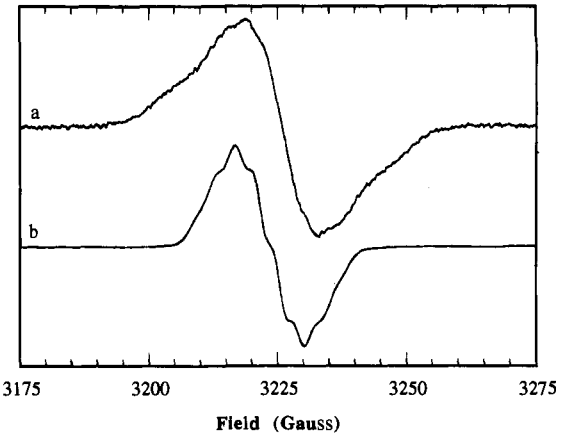

Figure 2. Fluid solution (298 K) EPR spectra of the sodium (a) and PPN (b) salts of the monoreduced radical anion $[Al(dpt)_3]^-$.

($A_\perp$) of the more strongly coupled nitrogen, and the line-broadening parameter were estimated by comparing experimental and simulated spectra. The strong couplings of the single nitrogen are quantitatively very similar to those found in nitroxide spin-labels, indicating that the majority of the electron spin density resides on this single, inequivalent nitrogen.

Error estimates for the weak EPR hyperfine couplings are difficult to obtain due to the broad spectral lines and the large number of independent parameters in the fit of the EPR spectrum; *i.e.*, a unique fit cannot be obtained. In order to obtain an estimate of the errors for the weakly coupled nitrogens, we have performed simulations of the EPR spectra for different weak nitrogen hyperfine couplings while fixing all the other fit parameters (*i.e.*, strongly coupled nitrogen and line width). A decrease of 15% in the hyperfine coupling to these weaker nitrogens results in a noticeable difference in the broad triplet line structure. Thus, the error in the EPR hyperfine couplings can be estimated as being less than ±15%.

In principle, this analysis could be bolstered by an examination of fluid solution spectra that are determined by the average couplings only. The $[Al(dpt)_3]^-$ anion, however, gives a poorly resolved fluid solution spectrum as is evident in Figure 2,[7] prompting isotope-labeling studies. Spectra of isotopic derivatives of $[Al(dpt)_3]^-$, in which either the flanking (1,3) or central (2) nitrogen positions are labeled with ^{15}N, provide additional conformation of the above results. The ^{15}N-labeled compounds $Al(dpt\text{-}2\text{-}^{15}N)_3$ (**II**) and $Al(dpt\text{-}1,3\text{-}^{15}N_2)_3$ (**III**) were prepared from the reaction of $AlMe_3$ with 3 equiv of the appropriately labeled triazenide ligand. The monoradical complexes $[Al(dpt\text{-}2\text{-}^{15}N)_3]^-$ and $[Al(dpt\text{-}1,3\text{-}^{15}N_2)_3]^-$ were prepared in a manner analogous to the "unlabeled" (all ^{14}N) complex $[Al(dpt)_3]^-$.

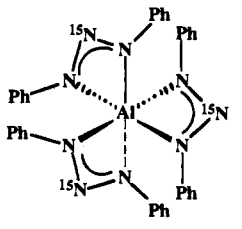

$Al(dpt\text{-}2\text{-}^{15}N)_3$ (II)

$Al(dpt\text{-}1,3\text{-}^{15}N_2)_3$ (III)

The frozen solution (77 K, THF) EPR spectra of the ^{15}N isotope-labeled monoanions $[Al(dpt\text{-}1,3\text{-}^{15}N_2)_3]^-$ and $[Al(dpt\text{-}2\text{-}^{15}N)_3]^-$ are shown in Figure 3 (spectral lines (b) and (c), respectively) along with the analogous spectra for the unlabeled complex, Figure 3a (*cf.*, Figure 1a). Despite the clear differences

(5) For recent reviews of multifrequency ESEEM, see: (a) Larsen, R. G.; Gerfen, G. J.; Singel, D. J. *Appl. Magn. Reson.* **1992**, *3*, 369. (b) Singel, D. J. In *Advanced EPR: Applications in Biology and Biochemistry*; Hoff, A. J., Ed.; Elsevier: Amsterdam, 1989; p 119. (c) Dikanov, S. A.; Tsvetkov, Y. D. *Electron Spin Echo Envelope Modulation Spectroscopy*; CRC Press: Boca Raton, FL, 1992.

(6) See, for example: (a) Griffith, O. H.; Cornell, D. W.; McConnell, H. M. *J. Chem. Phys.* **1965**, *43*, 2909. (b) Buettner, G. R. *Free Radical Biol. Med.* **1987**, *3*, 259 and references therein.

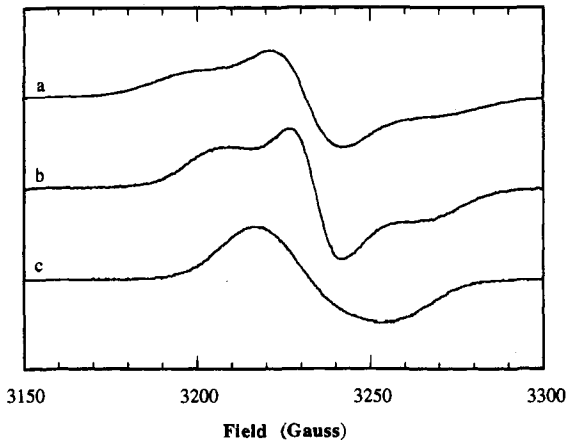

Figure 3. Frozen solution (77 K) EPR spectra of $[Al(dpt)_3]^-$ (a), $[Al(dpt\text{-}1,3\text{-}^{15}N_2)_3]^-$ (b), and $[Al(dpt\text{-}2\text{-}^{15}N)_3]^-$ (c).

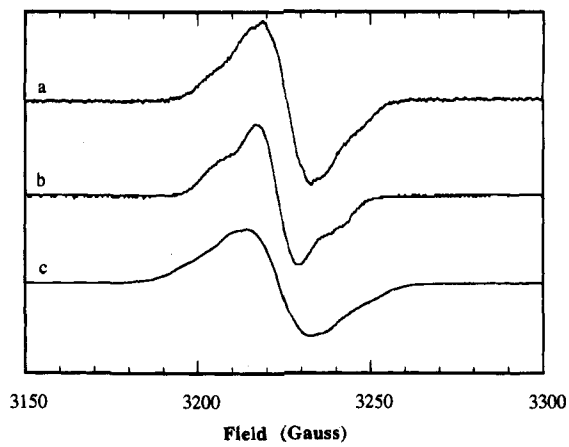

Figure 4. Fluid solution (298 K) EPR spectra of $[Al(dpt)_3]^-$ (a), $[Al(dpt\text{-}1,3\text{-}^{15}N_2)_3]^-$ (b), and $[Al(dpt\text{-}2\text{-}^{15}N)_3]^-$ (c).

in the spectra of the two types of labeled ligands, both spectra appear broad and poorly resolved, substantiating the notion that the coupling scheme is too complex to be attributed to a single nitrogen nucleus. A comparison of the spectra does confirm that a plurality of the electron spin density resides on the central nitrogen of the triazenide ligand. Thus, while the flanking ^{15}N-labeled spectrum (Figure 3b) displays a broad triplet line structure that is almost identical to that of the unlabeled sample (Figure 3a), the central ^{15}N-labeled sample (Figure 3c) displays a notably different line shape, in which the triplet structure is lost, as a consequence of the isotopic substitution. As shown in Figure 4, an analogous line-shape behavior is observed in the room-temperature fluid solution spectra for the various isotope-labeling combinations.

ESEEM Spectroscopy. The EPR spectra indicate that the radical obtained upon reduction is ligand-centered with a majority of the spin density residing on a single, central nitrogen of one of the three triazenide rings. They also suggest the possibility of a smaller, but still appreciable, spin density on a pair of nitrogens. The EPR data do not reveal whether these particular nitrogens are situated on the same ligand as the strongly coupled nitrogen, nor do they reveal the hyperfine interactions of the other six nitrogens. From the EPR data, it is not obvious that there exists "coherent" electron delocalization, and the identity of the weak couplings cannot be assigned. These issues are addressed by ESEEM spectroscopy.

(7) The lack of resolution may involve a number of different factors. First, it is possible that the anisotropic hyperfine interactions are not being averaged out in fluid solution due to slow rotational motion of the aluminum complex. However, an estimate of the rotational correlation time for the aluminum complex in THF at 298 K ($\tau_c \approx 1 \times 10^{-9}$ s) would suggest that this is not the case. See, for example: (a) Robinson, B.; Thomann, H.; Beth, A.; Fajer, P.; Dalton, L. R. In *EPR and Advanced EPR Studies of Biological Systems*; Dalton, L. R., Ed.; CRC Press: Boca Raton, FL, 1985; p 38. (b) Marsh, D.; Horvath, L. I. In *Advanced EPR: Applications in Biology and Biochemistry*; Hoff, A. J., Ed.; Elsevier: Amsterdam, 1989; p 707. The rotational correlation time, given by $4\pi\eta a^3/3kT$ (η = viscosity, a = radius, k = Boltzman constant, T = temperature) is derived from the Stokes–Einstein–Debye Theorem. See, for example: (c) Carrington, A.; McLachlan, A. D. *Introduction to Magnetic Resonance*; Harper & Row: New York, 1967; p 187. (d) Debye, P. J. W. *Polar Molecules*; Dover Publications: New York, 1945; Chapter 5. Second, the unpaired electron of the $[Al(dpt)_3]^-$ radical, while centered on a single triazenide at 77 K, may, at 298 K, be "hopping" from one ligand to the next, which could potentially lead to a broadening of the observed signal. Finally, the presence of spin–spin coupling to the sodium, aluminum, or additional nitrogen nuclei is a possible source of the line broadening. The similarity of the spectra for the Na and PPN salts precludes the presence of significant coupling between the sodium cation and the $[Al(dpt)_3]^-$ anion. Strong interaction with the aluminum is ruled out by the ESEEM spectroscopy, as discussed later, in which only a very weak coupling to the aluminum is observed. There is no evidence for any ligand exchange processes involving the triazenide ligands in any of our aluminum compounds.

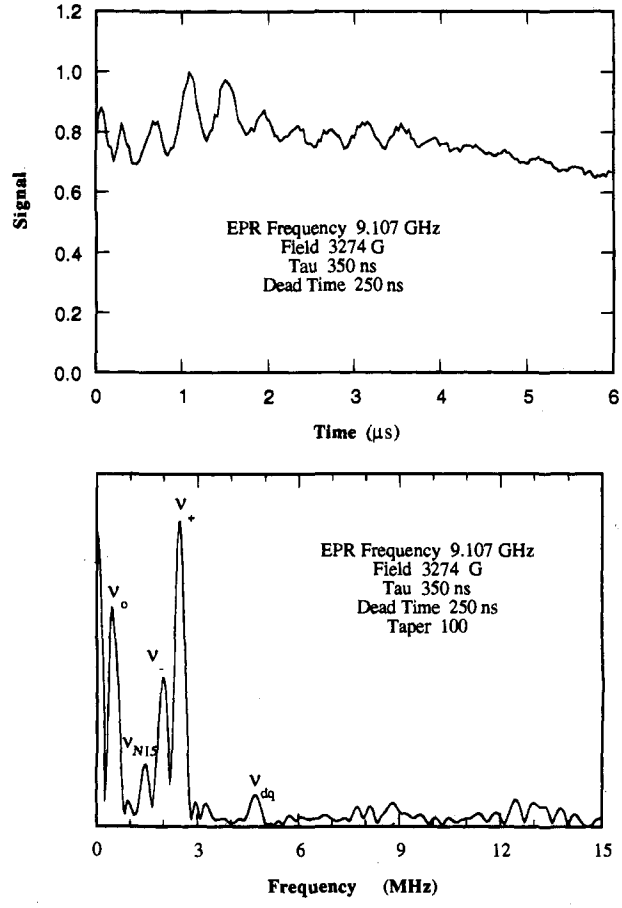

Figure 5. Three-pulse, time domain (upper) and magnitude Fourier transform (lower) ESEEM spectra of the radical anion $[Al(dpt\text{-}2\text{-}^{15}N)_3]^-$ acquired near exact cancellation. Evident in the lower spectra are features from both weakly coupled, central ^{15}N nuclei, giving rise to an ^{15}N Zeeman peak at 1.46 MHz, as well are pure ^{14}N quadrupolar peaks appearing at 0.46, 1.95, and 2.44 MHz, and an ^{14}N double quantum peak, at 4.72 MHz, arising from flanking nitrogen nuclei.

The ESEEM spectra of the sodium salts of $[Al(dpt)_3]^-$, $[Al(dpt\text{-}2\text{-}^{15}N)_3]^-$, and $[Al(dpt\text{-}1,3\text{-}^{15}N_2)_3]^-$ were collected at 77 K in THF frozen solution in a manner analogous to that previously described.[8] In Figure 5b is shown the three-pulse spectrum of the ^{15}N central-labeled complex $[Al(dpt\text{-}2\text{-}^{15}N)_3]^-$. Evident in this spectrum is a peak at the ^{15}N Zeeman frequency (ν_n = 1.46 MHz). Such peaks appear when the hyperfine

(8) Cosgrove-Larsen, S. A. Ph.D. Thesis, Harvard University, Cambridge, MA, 1992.

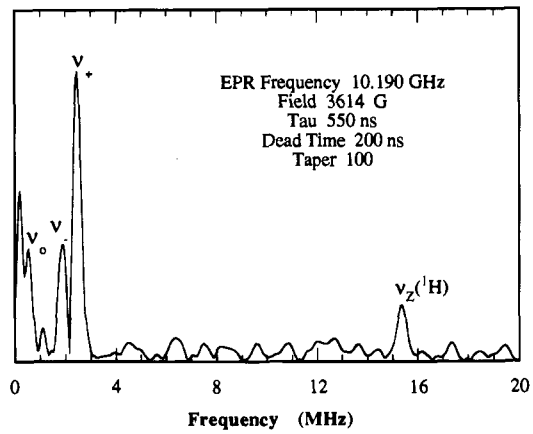

Figure 6. Three-pulse, magnitude Fourier transform ESEEM spectrum of the radical anion $[Al(dpt)_3]^-$ acquired near exact cancellation exhibiting an ^{14}N quadrupolar spectrum with peaks centered at 0.43, 1.88, and 2.46 MHz and a proton fundamental peak at 15.39 MHz. The ^{14}N "double quantum" peak observed in Figure 5 is no longer observed due to the τ "suppression" effect.

coupling is considerably smaller than the Zeeman interaction. Accordingly, the ^{15}N Zeeman peak cannot be assigned to the nitrogen that produces the large splitting in the EPR spectrum (Figure 1); rather, it is assigned to the central nitrogens on the other two ligands. These weakly coupled central nitrogens are not observed for the unlabeled complex $[Al(dpt)_3]^-$ (Figure 6), presumably because of the quadrupolar broadening of the analogous ^{14}N signal.

Ideally, one would like to simulate the ESEEM data shown in Figure 5b in order to distinguish the number of coupled nitrogen nuclei in cases where the isotope labeling is unable to do so. Simulations in the time domain are complicated by the many different couplings present; obtaining a unique fit in the time domain is often not possible. Simulation of the frequency domain peak amplitudes, which are a function of both the hyperfine coupling and the number of coupled nuclei, could in principle be used to determine the number of nuclei if an independent determination of the hyperfine coupling is available, *i.e.*, from the line widths or frequency-tracking data. For the very weakly coupled central nitrogens, evident as an ^{15}N Zeeman peak, the line width in three-pulse experiments (see Figure 5b) is dominated by the dipolar coupling and achieves a "first-order" line width of $^3/_2A_2^0 = 0.326$ MHz. Simulation of the ^{15}N Zeeman peak of Figure 5b for coupling to a single nucleus with $A_2^0 = 0.217$ MHz results in a peak amplitude that is half as intense as the experimental peak amplitude, indicating that we are observing coupling to two central ^{15}N nuclei.

The centrally labeled complex $[Al(dpt\text{-}2\text{-}^{15}N)_3]^-$ also exhibits a three-line quadrupolar spectrum, with peak frequencies of 0.46, 1.95, and 2.44 MHz, arising from ^{14}N ($I = 1$) flanking nitrogens. The quadrupolar nature of these lines is verified by multifrequency ESEEM; quadrupole peaks are observed only when the nuclear Zeeman and hyperfine interactions approximately cancel in one electron spin manifold.[9] From an analysis[10] of the quadrupolar peaks of $[Al(dpt\text{-}2\text{-}^{15}N)_3]^-$, we derive the quadrupole coupling constant $K = e^2qQ/4 = 0.70$ MHz and the asymmetry parameter $\eta = 0.44$. The ^{14}N isotropic hyperfine coupling can be estimated from the "cancellation" condition to be $A_0^0(^{14}N) = 2\nu_n \pm K \approx 2.0 \pm 0.7$ MHz. Similar quadrupolar spectra are exhibited in Figure 6 for the unlabeled sample $[Al(dpt)_3]^-$.

(9) Flanagan, H. L.; Singel, D. J. *J. Chem. Phys.* **1987**, *87*, 5606.
(10) (a) Flanagan, H. L.; Gerfen, G. J.; Singel, D. J. *J. Chem. Phys.* **1988**, *88*, 20. (b) Reijerse, E. J.; Keijzers, C. P. *J. Magn. Reson.* **1987**, *71*, 83.

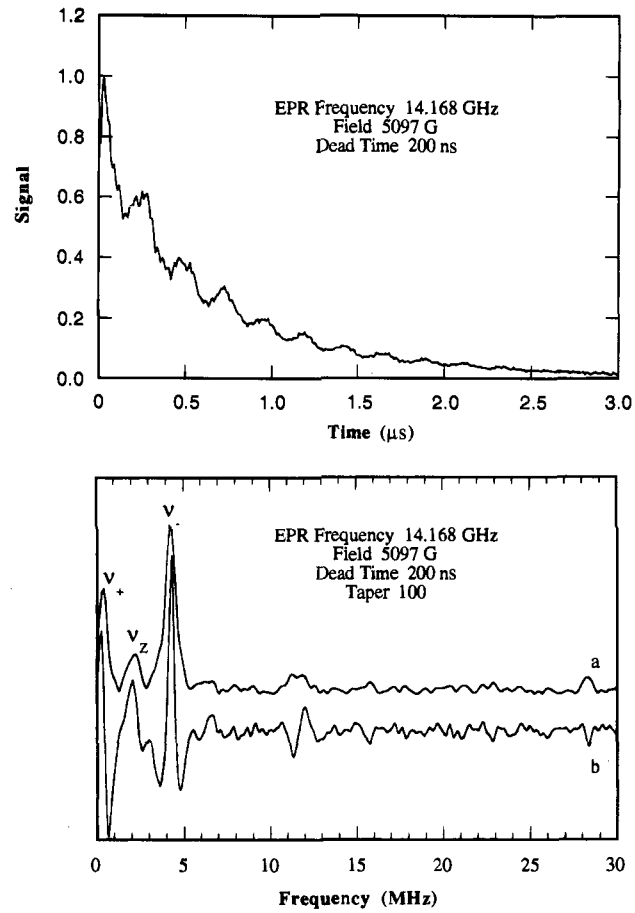

Figure 7. Two-pulse, time domain (upper), magnitude (lower, a), and cosine (lower, b) Fourier transform ESEEM spectra of the radical anion $[Al(dpt\text{-}1,3\text{-}^{15}N_2)_3]^-$. The spectral features at 0.29 and 4.30 MHz are assigned to weak, isotropically coupled, flanking ^{15}N nuclei. The peak appearing at the ^{15}N Zeeman frequency of 2.05 MHz is attributed to remote, anisotropically coupled, flanking ^{15}N nuclei.

A two-pulse ESEEM spectrum of $[Al(dpt\text{-}1,3\text{-}^{15}N_2)_3]^-$ (**III**) shown in Figure 7b immediately reveals two distinct types of flanking nitrogens. First, from nitrogen nuclei very weakly coupled to the electron spin, a peak at the ^{15}N Zeeman frequency (2.05 MHz) is evident. Second, from nitrogens with an appreciable hyperfine coupling, a pair of peaks (0.29 and 4.30 MHz) split about the ^{15}N Zeeman frequency is also seen. This latter coupling, approximate ^{15}N (^{14}N) hyperfine interactions of *ca.* 3.8 (2.7) MHz, can be associated with those flanking nitrogens that give rise to the ^{14}N quadrupolar spectrum in Figure 5. Precise values of the hyperfine coupling constants are readily obtainable *via* multifrequency ESEEM techniques of the type described by Gerfen and Singel.[11] In particular, the hyperfine coupling parameters can be determined through a frequency tracking of the high- (ν_-) and low- (ν_+) frequency ^{15}N fundamental peaks[12] with varying EPR excitation frequencies. The low-frequency peak exhibits an amplitude resonance when the magnitude of the Zeeman interaction is matched with the hyperfine coupling. Far from match, the linear relationship between the quantities ($\nu_\pm^2 - \nu_n^2$) and the ^{15}N Zeeman frequency (ν_n) allows one to extract the hyperfine coupling interaction matrix elements. As the match range is traversed, there are inflections away from the linear behavior due to the match condition being fulfilled at different orientations as the field/frequency is swept. The detailed shape of the frequency

(11) Gerfen, G. J.; Singel, D. J. *J. Chem. Phys.* **1994**, *100*, 4127.
(12) (a) Gerfen, G. J.; Singel, D. J. *J. Chem. Phys.* **1990**, *93*, 4571. (b) Gerfen, G. J. Ph.D. Thesis, Harvard University, Cambridge, MA, 1990.

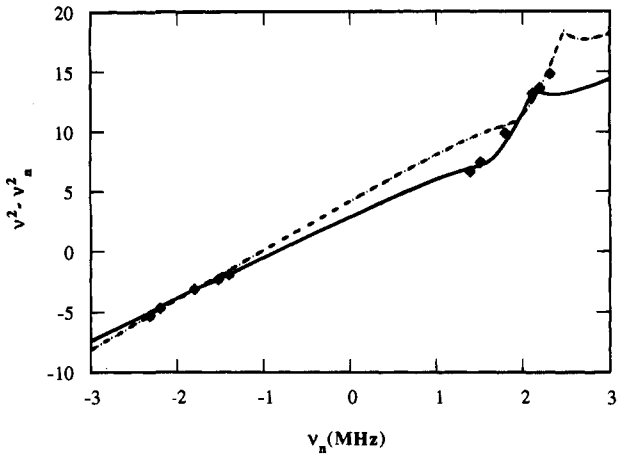

Figure 8. Frequency tracking of the Fermi contact-shifted ^{15}N ESEEM peaks of the $[Al(dpt\text{-}1,3\text{-}^{15}N_2)_3]^-$ radical anion. The diamonds (◆) correspond to experimentally measured two- and three-pulse modulation frequencies measured over a range of spectrometer excitation frequencies, from 9.1 to 14.8 GHz. The curves correspond to theoretically calculated peak frequencies for different hyperfine coupling parameters: (solid curve) $A_0^0 = 3.5$ MHz, $A_2^0 = 0.39$ MHz, and $\beta = A_0^0/A_2^0 > 0$, and (dashed curve) $A_0^0 = 4.2$ MHz, $A_2^0 = 0.39$ MHz, and $\beta > 0$.

tracks, the position and shape of the excursions from the asymptotic, linear behavior, depends sensitively on the values of A_0^0 and A_2^0. As summarized in Figure 8, however, no single set of hyperfine coupling parameters generates a theoretical curve that suits the present data. The simplest interpretation is to invoke the presence of two slightly inequivalent nitrogens with isotropic hyperfine couplings of 3.50 and 4.18 MHz. The average isotropic hyperfine coupling constant for these ^{15}N-flanking nitrogens, $A_0^0(^{15}N) = 3.84$ MHz, is consistent with the value of $A_0^0(^{14}N) = 2.0 \pm 0.7$ MHz, estimated from the cancellation condition, for the flanking ^{14}N nitrogens of the central ^{15}N-labeled complex $[Al(dpt\text{-}2\text{-}^{15}N)_3]^-$.[13]

Simulations of the two-pulse ESEEM spectra were performed to confirm the above interpretation. While in the two-pulse experiments of Figures 7b and 8 the line widths are typically no longer dominated by the dipolar relaxation but rather by the more rapid phase-memory relaxation time, an independent estimate of the hyperfine coupling can still be obtained for the more strongly coupled, flanking nitrogen nuclei ($A_0^0 = 1$ G) from the frequency-tracking data. Simulations of these ^{15}N nitrogen couplings were performed, and the analysis of both the line width and peak amplitudes supports the notion of coupling to two slightly inequivalent nuclei. The high-frequency ^{15}N peak does not achieve match under the experimental conditions and should therefore achieve at least its first-order dipolar line width of $^3/_2A_2^0 = 0.6$ MHz.[14] The observed experimental line width is only 0.3 MHz. Simulation of coupling to two slightly inequivalent nitrogens indicates that the ^{15}N high-frequency (ν_-) composite line can achieve a narrower line width due to destructive interference of fundamental peaks and antiphase combination troughs in cosine transform spectra.[15] Furthermore, the experimental signal amplitude is too large to be consistent with simulations of coupling to a single ^{15}N nucleus.

(13) The isotropic hyperfine couplings differ by approximately the ratio of the γ's: $\gamma(^{15}N)/\gamma(^{14}N) = 1.4$.

(14) Lai, A.; Flanagan, H. L.; Singel, D. J. *J. Chem. Phys.* **1988**, *89*, 7161.

(15) In two-pulse cosine spectra, one observes both fundamental frequencies as well as their sum and difference peaks. The combination peaks appear antiphase to the fundamental frequencies. See: Halkides, C. J.; Farrar, C. T.; Larsen, R. G.; Redfield, A. G.; Singel, D. J. *Biochemistry* **1994**, *33*, 4019.

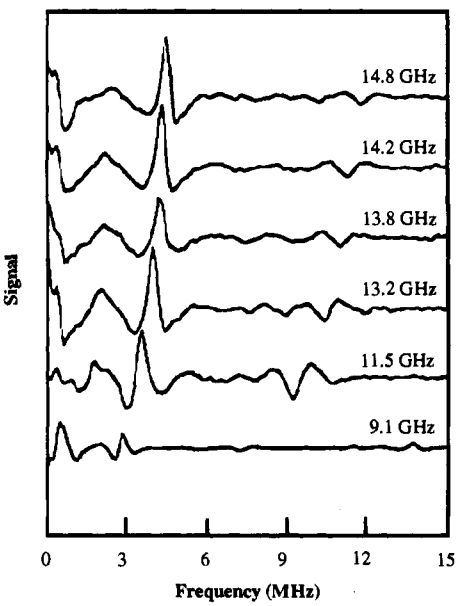

Figure 9. Stacked plot of two-pulse, cosine transform ESEEM spectra exhibiting the frequency tracking of the ^{15}N fundamental and ^{27}Al sum combination peak frequencies with varying spectrometer excitation frequency for the radical anion $[Al(dpt\text{-}1,3\text{-}^{15}N_2)_3]^-$. The EPR excitation frequency is varied from 9.1 to 14.8 GHz (bottom to top).

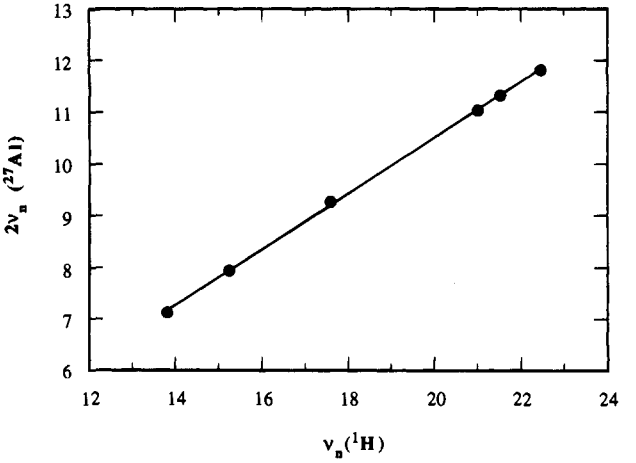

Figure 10. Frequency tracking of the aluminum sum combination peak with varying spectrometer excitation frequencies expressed as proton Zeeman peak frequencies. The solid line represents the best fit to the track of the experimental aluminum sum combination peak frequencies (solid circles) and has a slope that is proportional to the aluminum: proton γ ratio ($y = -0.278\,87 + 0.539\,51x$; $R = 0.999\,79$).

Figure 9 shows a stacked plot of two-pulse ESEEM spectra that show the ^{15}N peaks employed in the frequency-tracking plot of Figure 8. Also evident in these spectra is a higher frequency peak at twice the ^{27}Al Zeeman frequency (a sum combination peak). This peak frequency is plotted, in Figure 10, *vs* the proton Zeeman frequency. The slope of the straight line through the data is 0.54. This value corresponds extremely well with twice the ratio of the ^{27}Al and ^1H magnetic moments, namely 0.52 and thus confirms the assignment to ^{27}Al. There is no evidence of ^{27}Al fundamental peaks, suggesting anisotropic coupling to the ^{27}Al through which fundamental peaks are extensively broadened by frequency dispersive terms. These terms can cancel in the ^{27}Al sum combination peak, giving rise to a sharpened, observable signal.[5] Observation of this combination peak, as discussed previously by Matar and Goldfarb,[16]

(16) Matar, K.; Goldfarb, D. *J. Chem. Phys.* **1992**, *96*, 6464.

indicates that the ^{27}Al quadrupole-coupling interaction must be small since the ^{27}Al combination peak is extensively broadened by large quadrupole couplings. A quadrupole-coupling constant of 0.215 MHz and an asymmetry parameter of 0.802 were obtained from *ab initio* calculations of the electric field gradient at the aluminum nucleus. The observed weak coupling to the aluminum is consistent with the proposed ligand-centered nature of the aluminum radical anion complex.[17] Finally, we note that only very weak ^1H hyperfine couplings, manifested as peaks exclusively at ^1H Zeeman frequencies, are observed in the ESEEM spectra. Such weak couplings indicate that the spin density is not delocalized onto the phenyl rings of the triazenide ligands.

***Ab Initio* Calculations.** From the ESEEM and EPR spectra, we are able to distinguish five different types of hyperfine couplings. The EPR spectra resolve one strongly coupled ($A_{II}^{II} \approx 13$ G) central nitrogen and a pair of less strongly coupled ($A_{II}^{II} \approx 3$ G) flanking nitrogens. The ESEEM results reveal the presence of weaker couplings ($A_{II}^{II} \approx 1$ G) to a second type of flanking nitrogen and a very weak anisotropic coupling to a third type of flanking nitrogen and to the other two central nitrogens. From the experimental data, it cannot be determined which of the different flanking nitrogen couplings are situated on the same ligand as the unique, strongly coupled central nitrogen. The assignment of the flanking nitrogen couplings to specific positions is made possible by theoretical *ab initio* calculations performed on the monoreduced complex $[Al(HNNNH)_3]^-$ (**IV**) using the GAUSSIAN 90 suite of programs.

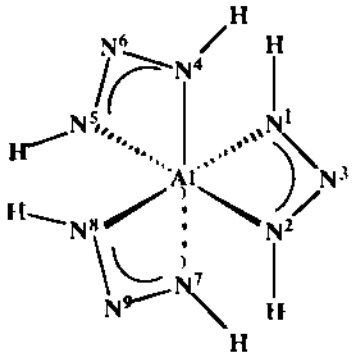

(IV)

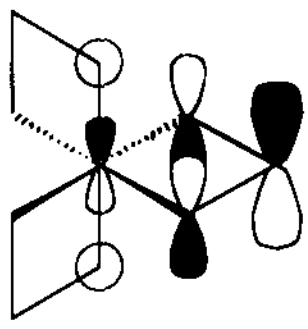

(V)

The hydrogen-substituted triazenide derivative was chosen in order to reduce the size of the calculation; however, the atomic coordinates were taken from X-ray crystallographic structure of $[Al(dpt)_3]^-$.[1] The idealized D_3 symmetry of the $Al(NNN)_3$ core of the $Al(dpt)_3$ molecule is broken in the crystal structure; one of the triazenide ligands is singled out by shorter Al−N and longer N−N bond lengths. For simplicity in further discussion, the various nitrogen nuclei have been numbered 1−9 (see **IV**), with the unique triazenide ligand containing N(1)−N(2)−N(3). The HOMO (highest occupied molecular orbital) atomic orbital coefficients and HOMO spin densities are given in Tables 1 and 2, respectively. Details of the calculative method are given in the Experimental Section.

From a consideration of the HOMO atomic orbital coefficients of $[Al(HNNNH)_3]^-$, a number of comparisons may be made with the EPR and ESEEM spectroscopic data, and subsequent assignment of the source of the observed experimental couplings is proposed.

(1) The unique ligand [N(1)−N(2)−N(3)] has *ca.* 75% of the electron spin density, indicative of a ligand-centered radical anion.

(2) The large s orbital spin density of the central nitrogen, N(3), of the unique, "reduced" triazenide is supportive of the dominant role of the central nitrogen observed in the EPR spectra (see Figure 3).

Table 1. HOMO Coefficients in $[Al(HNNNH)_3]^-$ at the 3-21G* Basis Set Level Calculated Using GAUSSIAN 90[a]

atom	atomic orbital	HOMO coefficients	atom	atomic orbital	HOMO coefficients
Al	3S (I)	0.050 66	N(1)	2S (I)	−0.010 70
	$3P_x$ (I)	0.005 78		$2P_x$ (I)	−0.011 42
	$3P_y$ (I)	0.123 47		$2P_y$ (I)	−0.203 64
	$3P_z$ (I)	0.002 16		$2P_z$ (I)	−0.002 16
	3S (O)	0.094 40		2S (O)	0.078 39
	$3P_x$ (O)	0.000 77		$2P_x$ (O)	−0.013 00
	$3P_y$	0.100 10		$2P_y$ (O)	−0.212 13
	$3P_z$ (O)	0.007 82		$2P_z$ (O)	−0.000 51
N(2)	2S (I)	0.014 29	N(3)	2S (I)	0.044 08
	$2P_x$ (I)	−0.036 38		$2P_x$ (I)	0.044 09
	$2P_y$ (I)	−0.227 26		$2P_y$ (I)	0.338 58
	$2P_z$ (I)	0.051 54		$2P_z$ (I)	−0.048 05
	2S (O)	0.051 11		2S (O)	0.246 25
	$2P_x$ (O)	−0.043 80		$2P_x$ (O)	0.054 59
	$2P_y$ (O)	−0.241 83		$2P_y$ (O)	0.387 84
	$2P_z$ (O)	0.064 00		$2P_z$ (O)	−0.062 63
N(4)	2S (I)	−0.011 41	N(5)	2S (I)	−0.007 13
	$2P_x$ (I)	−0.076 73		$2P_x$ (I)	−0.029 74
	$2P_y$ (I)	−0.006 85		$2P_y$ (I)	−0.063 16
	$2P_z$ (I)	0.015 28		$2P_z$ (I)	−0.030 17
	2S (O)	−0.080 28		2S (O)	−0.037 21
	$2P_x$ (O)	0.089 42		$2P_x$ (O)	−0.029 10
	$2P_y$ (O)	−0.003 93		$2P_y$ (O)	−0.081 94
	$2P_z$ (O)	0.018 56		$2P_z$ (O)	−0.036 54
N(6)	2S (I)	−0.001 39	N(7)	2S (I)	−0.011 97
	$2P_x$ (I)	0.069 43		$2P_x$ (I)	0.069 80
	$2P_y$ (I)	0.006 80		$2P_y$ (I)	−0.022 31
	$2P_z$ (I)	−0.020 02		$2P_z$ (I)	−0.008 59
	2S (O)	−0.043 90		2S (O)	−0.083 01
	$2P_x$ (O)	0.080 52		$2P_x$ (O)	0.080 73
	$2P_y$ (O)	0.002 85		$2P_y$ (O)	−0.023 95
	$2P_z$ (O)	−0.026 18		$2P_z$ (O)	−0.009 82
N(8)	2S (I)	−0.005 42	N(9)	2S (I)	−0.001 35
	$2P_x$ (I)	0.026 06		$2P_x$ (I)	−0.063 89
	$2P_y$ (I)	−0.050 38		$2P_y$ (I)	0.013 00
	$2P_z$ (I)	0.021 37		$2P_z$ (I)	0.020 36
	2S (O)	−0.026 39		2S (O)	−0.039 88
	$2P_x$ (O)	0.025 21		$2P_x$ (O)	−0.074 56
	$2P_y$ (O)	−0.065 36		$2P_y$ (O)	0.010 48
	$2P_z$ (O)	0.024 67		$2P_z$ (O)	0.026 16

[a] The atomic coordinates were taken from the X-ray crystal structure of $[Al](dpt)_3||PPN|\cdot 5(THF)$.[1] The outer and inner basis functions used to allow for more diffuse or contracted orbitals are denoted by (I) and (O), respectively.

(3) It is clear that the unpaired electron is not entirely localized on the central nitrogen of the unique ligand, but rather, its spin density is distributed in the nitrogen $2p_y$ atomic orbitals across all three nitrogens of the unique ligand (**V**). The HOMO $2p_y$ coefficients are roughly in the ratio 1:2:1 [N(1):N(2):N(3)], consistent with the observed EPR spectra, which are too complex to be attributed to coupling to a single nitrogen nucleus.

(4) The spin densities on the flanking nitrogens of the radical ligand [N(1) and N(2)] are too large to be responsible for the hyperfine coupling observed in the ESEEM spectroscopy. On the basis of the small contribution of the 2s spin density of the N(4) and N(7) nitrogens (see **IV**) to the HOMO (see Table 2), we propose that the coupling actually observed in the ESEEM spectrum arises from these weak, isotropically coupled nitrogen atoms on the neighboring triazenide ligands, cis to the reduced

(17) The nearest other aluminum nucleus in the crystal structure is more than ~10−12 Å distant. This distance is expected to be even greater in the more dilute frozen solution (1−5 mM); due to the $1/r^6$ weighting of contributions to the ESEEM signal amplitude, distant aluminum nuclei from neighboring molecules are unlikely to contribute significantly to the signal amplitude. The small spin density in the 3p orbital of the *ab initio* calculation further support to our claim that the coupling observed is intramolecular.

Table 2. HOMO Electron Spin Density Distribution[a]

atom	HOMO spin density ϱ_p	ϱ_s
Al	0.0250	0.0048
N(1)	0.0864	0.0363
N(2)	0.1101	0.0039
N(3)	0.2638	0.2634
N(4)	0.0006	0.0091
N(5)	0.0037	0.0013
N(6)	0.0064	0.0002
N(7)	0.0037	0.0084
N(8)	0.0001	0.0011
N(9)	0.0023	0.0004

[a] The p and s atomic orbital spin densities calculated from the HOMO atomic orbital coefficients are tabulated as ϱ_p and ϱ_s, respectively.

ligand. The *ab initio* calculations also reveal a slight difference in spin density on these cis nitrogens [N(4) and N(7) in **IV**] in agreement with the ESEEM frequency-tracking data, which suggested coupling to two slightly inequivalent nitrogens.

(5) From the *ab initio* calculations, it is evident that there is only negligible spin density on either the central nitrogens of the "unreduced" ligands [N(5) and N(8) in **IV**] or the nitrogen atoms *trans* to the reduced ligand [N(6) and N(9)], which is consistent with a very weak anisotropic coupling to these nitrogens observed in the ESEEM as an ^{15}N Zeeman peak.

(6) While the spin density localized on the radical ligand is concentrated mainly in the $2p_y$ atomic orbitals of the three radical nitrogens, a small spin density is also evident in the aluminum $3p_y$ atomic orbital, which is consistent with the weak coupling to the aluminum manifested in the ESEEM spectra as an ^{27}Al sum combination peak.

A simple pictorial representation of the HOMO, involving the $3p_y$ orbital of the aluminum and the $2p_y$ nitrogen orbitals of one triazenide ligand, is given in **V**. This localization of the radical is completely supported by our experimental results. This picture is reminiscent of a p−π* hydrocarbon radical with strong anisotropic coupling to the unqiue ligand nitrogens and weaker anisotropic coupling to the ^{27}Al. Four of the nitrogens from the other ligands are either scarcely coupled (central and trans-flanking) or are, in effect, hyperconjugated to the π radical (cis flanking nitrogens) and thus sustain a predominantly isotropic coupling.

Finally, it is important to emphasize that we have taken the calculational coordinates from the X-ray crystal structure of $[Al(dpt)_3]^-$.[1] Even very small distortions of the molecular symmetry have been shown,[18] in *ab initio* calculations, to cause localization of the electron spin density onto the unique ligand, as opposed to a coherent delocalization over all ligands. Thus, it is not surprising that the distorted crystal geometry chosen enforces the localization of the electron spin density in the *ab initio* calculation. The exact source of this structural distortion is, at this point, not clear but may be due to a Jahn−Teller effect[19] in which the symmetric configuration of atoms, with electronic orbital degeneracy, is unstable with respect to an asymmetric displacement of the coordinates, thereby lifting the degeneracy. The distorted geometry could also be due to packing forces in the frozen solution and the crystal. Further, more detailed calculations would be required to estimate the magnitude of these interactions to determine which is the source of the distorted geometry. In as much as the calculated results, based on the crystal structure, are consistent with the experimental results performed in frozen solution, we suggest that the structural distortions in the two cases are similar.

Conclusion

Together, the EPR and ESEEM spectroscopies, and *ab initio* calculations provide a coherent understanding of the spin density distribution in the aluminum radical anion complex $[Al(dpt)_3]^-$. The HOMO of the radical is essentially triazenide N_3−π* in nature. The EPR spectra suggest localization of the radical electron spin density onto a single triazenido ligand, with the majority of the spin density residing on the central, strongly coupled nitrogen and two equivalent, more weakly coupled flanking nitrogens. This is confirmed by the EPR of the ^{15}N isotopic labeling of the 1 and 3 positions of the triazenide ligands, the ESEEM spectra of the central ^{15}N-labeled (2 position) and unlabeled compounds, and the HOMO orbital coefficients from *ab initio* calculations. The spin densities located on the flanking nitrogens of the radical ligand are too large to be responsible for the hyperfine coupling observed in the ESEEM spectrum of $[Al(dpt\text{-}1,3\text{-}^{15}N_2)_3]^-$; therefore, we propose that this coupling arises from a weak isotropic coupling to two of the nitrogen atoms on the neighboring unreduced triazenide ligands, specifically those cis to the reduced triazenide ligand. *Ab initio* calculations reveal a slight difference in spin density on these cis nitrogens in agreement with the experimental ESEEM data, which suggested coupling to two slightly inequivalent nitrogens. There appears to be only negligible spin density on either the central nitrogens of the unreduced ligands or the nitrogen atoms trans to the reduced ligand. Finally, while the spin density localized on the radical ligand is concentrated mainly in the 2p atomic orbitals of the three radical ligand nitrogens, a small spin density is also evident in the aluminum 3p atomic orbital, which is consistent with the weak coupling to the aluminum observed in the ESEEM as an ^{27}Al sum combination peak.

We have previously proposed[20] and presented theoretical[21] and photoelectron spectroscopic evidence[22] for the presence of electron donation from π-donor ligands (alkoxides and aryl oxides) to four-coordinate aluminum. The presence of weak coupling of the unpaired electron on the triazenide radical with both the aluminum center and the triazenide nitrogens cis to the reduced ligand is consistent with, and further evidence for, the presence of π-type interactions involving coordinatively saturated aluminum centers.

Experimental Section

All general experimental details and procedures including compound preparation, solvent purification, and sample preparation were carried out as described in the preceding paper.[1] $Na^{15}NO_2$ (MSD Isotopes, 99% ^{15}N) and $Ph^{15}NH_2$ (Cambridge Isotopes Labs, 99% ^{15}N) were used as received. THF was distilled from sodium−benzophenone ketyl solution immediately before use and further degassed by three freeze−pump−thaw cycles. All spectroscopic samples were prepared in a standard inert-atmosphere drybox equipped with a recirculating gas purifier. The THF solution samples prepared for EPR and ESEEM spectroscopy were in the $(1-5) \times 10^{-3}$ mol L^{-3} concentration range. Samples for the ESEEM spectroscopy were flame sealed under vacuum in quartz EPR tubes and stored in liquid N_2 to maintain their integrity throughout the course of the measurements.

(18) Farrar, C. T.; Singel, D. J. Unpublished results.

(19) (a) Ham, F. S. *Int. J. Quantum Chem.* **1971**, *5*, 191. (b) Ham, F. S. In *Electron Paramagnetic Resonance*; Geschwind, S., Ed.; Plenum Press: New York, 1972. (c) Van Vleck, J. H. *J. Chem. Phys.* **1938**, *7*, 61. (d) Van Vleck, J. H. *J. Chem. Phys.* **1938**, *7*, 72.

(20) Healy, M. D.; Wierda, D. A.; Barron, A. R. *Organometallics* **1988**, *7*, 2543.

(21) Barron, A. R.; Dobbs, K. D.; Francl, M. M. *J. Am. Chem. Soc.* **1991**, *113*, 39.

(22) (a) Lichtenberger, D. L.; Hogan, R. H.; Healy, M. D.; Barron, A. R. *J. Am. Chem. Soc.* **1990**, *112*, 3369. (b) Lichtenberger, D. L.; Hogan, R. H.; Healy, M. D.; Barron, A. R. *Organometallics* **1991**, *10*, 609.

Hdpt-2-^{15}N.[23] 1,3-Diphenyltriazine with the central nitrogen atom labeled (2-^{15}N) was prepared by the standard method,[24] employing $Na^{15}NO_2$ as the source of the isotopic label.

Hdpt-1,3-$^{15}N_2$. 1,3-Diphenyltriazene with the terminal nitrogen atoms labeled (1,3-$^{15}N_2$) was prepared by the standard method, employing $Ph^{15}NH_2$ as the source of the isotopic label.

Al[dpt-2-^{15}N]$_3$ was prepared from Hdpt-2-^{15}N in a fashion similar to that previously described for Al(dpt)$_3$,[25] with the modification that hexane was used in place of toluene to give a solvent-free product. NMR (C_6D_6, δ): ^{15}N, 88.7 (s, 2-*N*).

Al[dpt-1,3-$^{15}N_2$]$_3$ was prepared as above for Al[dpt-2-^{15}N]$_3$ using Hdpt-1,3-^{15}N. NMR (C_6D_6, δ): ^{15}N, −111.4 (s, 1,3-*N*).

EPR Spectroscopy. All continuous-wave (CW) EPR spectra were acquired at *ca.* 9.2 GHz on a Varian E-109 spectrometer interfaced through a Stanford Research Systems module (SR245) to an IBM PC. Low-temperature measurements, ranging from 77 to 110 K, were achieved with the use of a commercially available finger dewar insert or a nitrogen gas flow cryostat designed for the Varian cavity.

ESEEM Spectroscopy. A home-built ESEEM spectrometer, described previously,[26] was used to acquire all the spin-echo modulation patterns. Two- and three-pulse ESEEM experiments were performed at excitation frequencies of 9.1, 11.5, 13.2, 13.8, 14.2, and 14.8 GHz using four different three-loop, two-gap resonators. The two-pulse spin-echo modulation patterns consisted of 256 points acquired at 15 ns intervals with a 250 Hz repetition rate. Three-pulse experiments consisted of 300 points acquired with a 30 ns step size. Phase cycling of the pulses was employed to obtain measurement dead times less than τ. ESEEM patterns were acquired at each frequency *via* irradiation at the center of the EPR line, resulting in nominally orientationally nonselective spectra.[11,27] Typical duration of the $\pi/2$ pulse at the X band was 20 ns (Litton TWTA, Model 624, 8-18 GHz, 1 kW). All ESEEM experiments were performed at 77 K through the use of a low-temperature cryostat (Andonian Cryogenics). The magnetic field was calibrated with a Micro-Now Instruments model 515B-1 gaussmeter. Spectral analysis was carried out on an IBM PC employing a program described elsewhere.[28] The modulation patterns were fit to a Lorentzian, Gaussian, or polynomial decay function that was subsequently subtracted from the data. To mitigate dead time artifacts, the data were tapered with an extended cosine-bell function and zero-filled to 512 data points prior to fast Fourier transformation.

***Ab Initio* Calculations.** The *ab initio* all-electron molecular orbital calculations were performed on a Stardent P3000 computer using the UHF/3-21G* basis set of the GAUSSIAN 90 suite of programs. The UHF/3-21G* basis set has been found to provide good descriptions of the structures of organoaluminum compounds.[21] The UHF/3-21G* basis set consists of a double-ζ basis set in which two functions (more diffuse, O = outer, and contracted, I = inner, atomic orbitals) are used for each of the valence functions, allowing for added variational flexibility in the orbital exponents and introducing an extra degree of anisotropy, relative to the STO-3G basis set, to the orbitals.[29] The coordinates for the Al(NNN)$_3$ core structure were taken from the X-ray structure determination of [Al(dpt)$_3$]$^-$.[1] To reduce the size of the calculation, the phenyl rings of the triazenide ligands were replaced by protons that were restrained to lie in the ligand N_3 plane. For the model radical complex [Al(NNN)$_3$]$^-$, the value of $S^2 = S(S + 1)$ for the calculation was found to be 0.7501 ($S = {}^1/_2$). Since in the present study we are seeking not the prediction of absolute structures but rather a qualitative explanation for the observed spectral features, and taking into account the limits of computer time, we do not feel the application of a larger basis set is warranted.

Acknowledgment. This work was funded in part by a grant from the Aluminum Research Board. We are grateful to Richard Miller (Akzo Chemicals) for the gift of $AlMe_3$. We are grateful to both Dr. J. Evenseck, for assistance with the *ab initio* calculations, and Professor Martin Karplus, for allowing us access to his Stardent computer.

JA940577E

(23) (a) Kübler, R.; Lütke, W.; Weckerlin, S. *Z. Elektrochem.* **1960**, *64*, 650. (b) Clausias, K. *Angew. Chem.* **1955**, *66*, 497.

(24) Hartman, W. W.; Dickey, J. B. *Org. Synth.* **1943**, *2*, 163.

(25) Leman, J. T.; Barron, A. R.; Ziller, J. W.; Kren, R. M. *Polyhedron* **1989**, *8*, 1909.

(26) Cosgrove, S. A.; Singel, D. J. *J. Phys. Chem.* **1990**, *94*, 2619.

(27) Braunschweiler, L.; Schweiger, A.; Fauth, J. M.; Ernst, R. R. *J. Magn. Reson.* **1985**, *64*, 160.

(28) Larsen, R. Ph.D. Thesis, Harvard University, Cambridge, MA, 1992.

(29) (a) Hehre, W. J.; Radom, L.; Schleyer, P. v. R.; Pople, J. A. *Ab Initio Molecular Orbital Theory*; John Wiley: New York, 1986. (b) Szabo, A.; Ostlund, N. S. *Modern Quantim Chemistry*; McGraw-Hill Publishing Co.: New York, 1989.